

## Influence of cyclic aging on adhesive mode mixity in dissimilar composite/metal double cantilever beam joints

Moazzami, Mostafa; Ayatollahi, Majid R.; Akhavan-Safar, Alireza; Teixeira De Freitas, Sofia; Poulis, Johannes A.; da Silva, Lucas F.M.

**DOI**

[10.1177/14644207221074696](https://doi.org/10.1177/14644207221074696)

**Publication date**

2022

**Document Version**

Final published version

**Published in**

Proceedings of the Institution of Mechanical Engineers, Part L: Journal of Materials: Design and Applications

**Citation (APA)**

Moazzami, M., Ayatollahi, M. R., Akhavan-Safar, A., Teixeira De Freitas, S., Poulis, J. A., & da Silva, L. F. M. (2022). Influence of cyclic aging on adhesive mode mixity in dissimilar composite/metal double cantilever beam joints. *Proceedings of the Institution of Mechanical Engineers, Part L: Journal of Materials: Design and Applications*, 236(8), 1476-1488. <https://doi.org/10.1177/14644207221074696>

**Important note**

To cite this publication, please use the final published version (if applicable).  
Please check the document version above.

**Copyright**

Other than for strictly personal use, it is not permitted to download, forward or distribute the text or part of it, without the consent of the author(s) and/or copyright holder(s), unless the work is under an open content license such as Creative Commons.

**Takedown policy**

Please contact us and provide details if you believe this document breaches copyrights.  
We will remove access to the work immediately and investigate your claim.

***Green Open Access added to TU Delft Institutional Repository***

***'You share, we take care!' - Taverne project***

***<https://www.openaccess.nl/en/you-share-we-take-care>***

Otherwise as indicated in the copyright section: the publisher is the copyright holder of this work and the author uses the Dutch legislation to make this work public.

# Influence of cyclic aging on adhesive mode mixity in dissimilar composite/metal double cantilever beam joints

Proc IMechE Part L:  
*J Materials: Design and Applications*  
2022, Vol. 236(8) 1476–1488  
© IMechE 2022  
Article reuse guidelines:  
sagepub.com/journals-permissions  
DOI: 10.1177/14644207221074696  
journals.sagepub.com/home/pil



Mostafa Moazzami<sup>1</sup>, Majid R Ayatollahi<sup>1</sup> ,  
Alireza Akhavan-Safar<sup>2</sup>, Sofia Teixeira De Freitas<sup>3</sup>,  
Johannes A Poulis<sup>3</sup> and Lucas FM da Silva<sup>4</sup>

## Abstract

The adhesive layer in the adhesive joints can experience different modes of loading. Although the fracture energy of adhesive is generally considered to be a material parameter, it is found to be a function of the joint configuration too. Thus, to accurately simulate the behaviour of bonded joints, it is recommended to obtain the fracture energy of the joints using the same substrate(s) as in real applications. In some applications, it is necessary to join dissimilar substrates using adhesives. However, for pure mode fracture tests it is essential to reach the desired loading mode even in a dissimilar joint. Not only the joint configuration but also the environmental conditions need to be considered in fracture tests. In this condition, due to the aging, the stiffness of substrates and adhesive layer might change, and as a result, the adhesive may experience a mixed-mode loading condition. The current study aims to investigate the variation of the mode mixity for dissimilar double cantilever beam adhesive joints with composite/metal substrates subjected to cyclic aging. At different stages of the aging cycles, the mode mixity was calculated during the test using displacement fields obtained by digital image correlation and based on the Williams series expansion. In addition, the variation of flexural stiffness of polymer matrix composite substrates after cyclic aging was investigated using a three-point bending test. Finally, based on the variation of composite substrate flexural stiffness and using the finite element method, the variation of the mode-mixity ratio was calculated numerically and compared to the experimental results. The obtained results show that during the cyclic aging the moisture diffusion decreases flexural stiffness of polymer matrix composite substrates significantly, but the variation of substrate flexural stiffness deviates the mode mixity in the aged double cantilever beam specimens.

## Keywords

Adhesives, mode mixity, adhesive joints, dissimilar double cantilever beam, cyclic aging

Date received: 24 November 2021; accepted: 22 December 2021

## Introduction

One of the most important advantages of adhesives is the possibility of bonding different materials such as metals, composites, and plastic. Fiber-reinforced polymer (FRP) composites have attracted the most attention as a profitable material in different industries.<sup>1,2</sup> Widespread application of FRP laminates and metal structures simultaneously generated considerable recent research interest in the fields of FRP/metal adhesive joints.<sup>3–6</sup>

One of the fundamental issues for fracture analysis in adhesive joints is the concept of fracture energies.<sup>7–11</sup> Previous scientists proposed double cantilever beam (DCB) specimens with similar substrates for calculation of the mode I fracture energy of adhesive.<sup>12,13</sup> The difference in the material substrate fatigue and fracture behaviour of adhesive joints made from dissimilar adherends is more complex in comparison to adhesive joints made from similar adherends.<sup>14</sup> In dissimilar DCB adhesive

joints, the achievement of pure mode I loading is a challenging issue. There are some investigations in which researchers studied different methods to achieve pure mode I in dissimilar DCB specimens. For instance,

<sup>1</sup>Fatigue and Fracture Research Laboratory, Center of Excellence in Experimental Solid Mechanics and Dynamics, School of Mechanical Engineering, Iran University of Science and Technology, Iran

<sup>2</sup>Institute of Science and Innovation in Mechanical and Industrial Engineering (INEGI), Portugal

<sup>3</sup>Structural Integrity & Composites Group, Faculty of Aerospace Engineering, Delft University of Technology, the Netherlands

<sup>4</sup>Department of Mechanical Engineering, Faculty of Engineering, University of Porto, Portugal

### Corresponding author:

Majid R Ayatollahi, Fatigue and Fracture Research Laboratory, Center of Excellence in Experimental Solid Mechanics and Dynamics, School of Mechanical Engineering, Iran University of Science and Technology, Tehran, Iran.  
Email: m.ayat@iustac.ir

scientists used the criterion based on equality of the flexural stiffness of two substrates to obtain pure mode I loading.<sup>15–18</sup> Some investigators<sup>15,16</sup> have claimed that in this kind of designed dissimilar DCB adhesive joints, there are some shear stresses in the adhesive layer and the flexural stiffness-based criterion is not accurate to obtain pure mode I loading in dissimilar DCB joints.

Wang et al.<sup>16</sup> presented a new design criterion to obtain pure mode I loading in dissimilar DCB adhesive joints which are based on the equality of the longitudinal strain distribution at the interface of the substrates. The results of some investigations<sup>16,19</sup> show that matching the longitudinal strain distribution in dissimilar DCB spe-

exposed to cyclic aging is investigated. For this purpose, dissimilar DCB specimens with CFRP/aluminium substrates were made according to the longitudinal strain distribution criterion. Then, DCB specimens were exposed to cyclic aging and after a different number of aging cycles, the specimens were tensile tested. Using the DIC technique, the mode mixity of the un-aged and aged DCB joints was calculated. To determine the mode mixity, the ratio of SIFs ( $K_{II} / K_I$ ) was calculated during the tensile tests. To this end, the displacement fields were calculated using the DIC approach. Then, by an over-deterministic method which, is called the digital image correlation over-deterministic (DICOD) approach,

$$\begin{aligned} \begin{Bmatrix} \sigma_x \\ \sigma_y \\ \tau_{xy} \end{Bmatrix} &= \sum_{n=1}^{\infty} \frac{n}{2} A_n r^{\left(\frac{n}{2}-1\right)} \begin{Bmatrix} \left(2 + \frac{n}{2} + (-1)^n\right) \cos\left(\frac{n}{2}-1\right)\theta - \left(\frac{n}{2}-1\right) \cos\left(\frac{n}{2}-3\right)\theta \\ \left(2 - \frac{n}{2} - (-1)^n\right) \cos\left(\frac{n}{2}-1\right)\theta + \left(\frac{n}{2}-1\right) \cos\left(\frac{n}{2}-3\right)\theta \\ \left(\frac{n}{2}-1\right) \sin\left(\frac{n}{2}-3\right)\theta - \left(\frac{n}{2} + (-1)^n\right) \sin\left(\frac{n}{2}-1\right)\theta \end{Bmatrix} \\ &\quad - \sum_{n=1}^{\infty} \frac{n}{2} B_n r^{\left(\frac{n}{2}-1\right)} \begin{Bmatrix} \left(2 + \frac{n}{2} - (-1)^n\right) \sin\left(\frac{n}{2}-1\right)\theta - \left(\frac{n}{2}-1\right) \sin\left(\frac{n}{2}-3\right)\theta \\ \left(2 - \frac{n}{2} + (-1)^n\right) \sin\left(\frac{n}{2}-1\right)\theta + \left(\frac{n}{2}-1\right) \sin\left(\frac{n}{2}-3\right)\theta \\ -\left(\frac{n}{2}-1\right) \cos\left(\frac{n}{2}-3\right)\theta + \left(\frac{n}{2} - (-1)^n\right) \cos\left(\frac{n}{2}-1\right)\theta \end{Bmatrix} \end{aligned} \quad (1)$$

cimens is a general and more accurate approach to achieve pure mode I.

The investigation of the mode mixity of brittle materials is an approach proposed by some authors. One of them is based on the mode I and II stress intensity factors (SIFs).<sup>20</sup> Ayatollahi and Nejati<sup>20</sup> showed that the mode I and II SIFs can be obtained using an over-deterministic approach based on Williams series expansion. They measured these parameters by fitting the displacement fields with the Williams series expansion in different points near the crack tip.

In many applications of dissimilar adhesive joints with polymer matrix composite/metal substrates such as marine structures<sup>21</sup> and shipbuilding,<sup>1</sup> these joints are exposed to environments with different humidity levels. In aging conditions, polymer matrix composite and adhesive absorb moisture and as a result, the mechanical and chemical properties of them change significantly.<sup>22–25</sup> In addition, aging can create dimensional variations in polymer matrix composite substrates, known as hygrothermal effects.<sup>26</sup> Previous research showed that the fiber/matrix interface bonding can be affected by moisture uptake.<sup>27,28</sup> Compared to monotonous aging, studies on cyclic aging for the composite are relatively rare. However, a few scientists have studied the variation of the mechanical behaviour of composite material as a substrate in adhesive joints after cyclic aging.<sup>29,30</sup>

In this study, the mode-mixity variation of dissimilar DCB specimens with CFRP/aluminium substrates

modes I and II SIFs were obtained. In the numerical section, the variation of the mode-mixity before and after aging was calculated numerically. Finally, the experimental results were successfully compared with numerical results.

## Theoretical background

### Calculation of SIFs using an over-deterministic technique

In the cracked components, which are subjected to in-plane loading, the distribution of the linearly elastic stresses in front of the crack tip can be expressed using the Williams series expansion.<sup>31</sup> These equations can be written as follows:

where  $\theta$  and  $r$  are the polar coordinates of points near the crack tip, as illustrated in Figure 1,  $n$  is the coefficients order, and  $A_n$  and  $B_n$  are the coefficients relating to the modes I and II loadings, respectively. For calculation of modes I and II SIFs ( $K_I$  and  $K_{II}$ , respectively), the first coefficient in the Williams series expansion (i.e.  $n=1$ ), can be used. Equation (2) shows the described relations

$$K_I = \sqrt{2\pi}A_1, \quad K_{II} = \sqrt{2\pi}B_1 \quad (2)$$

As can be seen from equation (2), modes I and II SIFs can be obtained using the stress distribution around the crack tip. In addition, the SIFs can be calculated using

the Williams series expansion, based on the displacement distribution near the crack tip. Equations (3) and (4) present the relations between the displacement fields and the constant coefficients of the mode I and II loadings ( $A_n$  and  $B_n$ ).

$$\begin{aligned}
 u(r, \theta) &= \sum_{n=0}^N \frac{1}{2G} A_n r^{\frac{n}{2}} \times \left\{ \left( k + \frac{n}{2} + (-1)^n \right) \cos \frac{n}{2} \theta - \frac{n}{2} \cos \left( \frac{n}{2} - 2 \right) \theta \right\} \\
 &\quad + \sum_{n=0}^M \frac{1}{2G} B_n r^{\frac{n}{2}} \times \left\{ \left( -k - \frac{n}{2} + (-1)^n \right) \sin \frac{n}{2} \theta + \frac{n}{2} \cos \left( \frac{n}{2} - 2 \right) \theta \right\} \\
 &= f_0 A_0 + \sum_{n=1}^N A_n f_n^1(r, \theta) + \sum_{n=1}^M B_n f_n^2(r, \theta)
 \end{aligned} \quad (3)$$

$$\begin{aligned}
 v(r, \theta) &= \sum_{n=0}^N \frac{1}{2G} A_n r^{\frac{n}{2}} \times \left\{ \left( k - \frac{n}{2} - (-1)^n \right) \sin \frac{n}{2} \theta + \frac{n}{2} \cos \left( \frac{n}{2} - 2 \right) \theta \right\} \\
 &\quad + \sum_{n=0}^M \frac{1}{2G} B_n r^{\frac{n}{2}} \times \left\{ \left( k - \frac{n}{2} + (-1)^n \right) \cos \frac{n}{2} \theta + \frac{n}{2} \cos \left( \frac{n}{2} - 2 \right) \theta \right\} \\
 &= g_0 B_0 + \sum_{n=1}^N A_n g_n^1(r, \theta) + \sum_{n=1}^M B_n g_n^2(r, \theta)
 \end{aligned} \quad (4)$$

where  $u(r, \theta)$  and  $v(r, \theta)$  are the horizontal and vertical displacements, respectively, as shown in Figure 1.  $E$  and  $\nu$  are the elastic modulus and Poisson's ratio, respectively. In these expansions,  $G = E/2(1 + \nu)$  is the shear modulus,  $k$  is a constant parameter equal to  $(3 - 4\nu)$  for plane stress and  $(3 - \nu)/(1 + \nu)$  for plane strain conditions, and  $f_n^1(r, \theta)$ ,  $f_n^2(r, \theta)$ ,  $g_n^1(r, \theta)$ ,  $g_n^2(r, \theta)$  are functions which are constant at each point. It should be considered that, before using the displacement fields, the rotation and rigid body motions should be omitted from the deformations. In equations (3) and (4), the horizontal and vertical rigid body motions correspond to coefficients of  $A_0$  and  $B_0$ , respectively. Also, the rotation is represented by  $B_2$  in the Williams series expansion.

To obtain the displacement fields around the crack tip in the adhesive layer, the DIC method is considered in combination with the FEM. Using these approaches, a large number of data points, including polar coordinates and their horizontal and vertical displacements, were obtained. Therefore, for the calculation of mode I and II SIFs based on the Williams series expansion, an over-deterministic method was proposed. After calculation of the displacement fields near the crack tip, some data points were used as the input data for the over-deterministic technique. By fitting the level of displacements obtained from the DIC technique and the FEM to

the Williams series expansion (equations (3) and (4)), the first coefficients of the expansion can be calculated. The same approach was used to match the displacement fields for both the DIC and FEM results to the Williams series expansion. The absolute displacement values

obtained with DIC can, however, deviate from the results of the FEM. The displacement fields obtained by the DIC method are based on real conditions, while a certain simplification in the FEM leads to errors in the values obtained. Some phenomena such as residual stresses and test and manufacturing errors affect the DIC results while they are not taken into account in the FEM simulation. In order to investigate the real condition of aged samples and to analyse the possible effects of residual stresses and manufacturing errors, the mode-mixity variations obtained with DIC and FE methods

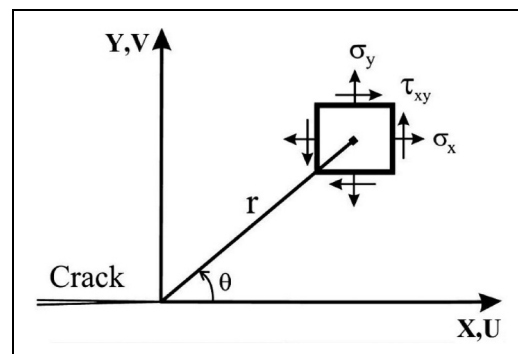
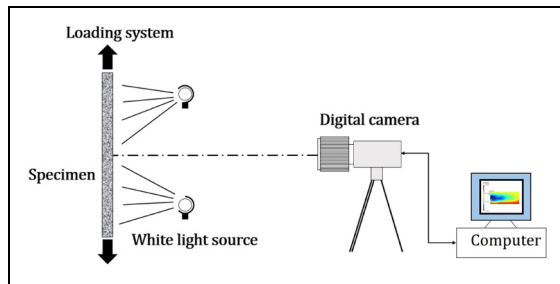


Figure 1. Crack tip stresses in a Cartesian coordinate system.



**Figure 2.** Typical experimental setup for the digital image correlation (DIC).

were compared. In this study, to calculate SIFs based on DIC and FEM results, a large number of data points was applied by considering ( $N=5$ ,  $M=5$ ) in equations (3) and (4), respectively. Ayatollahi and Nejati<sup>20</sup> used the over-deterministic method based on the Williams series expansion to calculate SIFs of cracked specimens. They concluded that the SIFs obtained using the over-deterministic method based on the Williams series expansion are in good agreement with the analytical or numerical results published in earlier papers.

The zone selected ahead of the crack tip where the data points are taken play an important role in the results since the linear elastic fracture mechanics (LEFM) assumption should be valid for the points selected. Since the Williams solution is based on the LEFM theory, the points used in this equation should be far enough from the crack tip to make sure they experience elastic deformations.

### DIC method

The DIC technique is an optical method for the calculation of displacement fields using the comparison of captured images. In this approach, the images should be captured before and after loading the specimen using a digital camera. The correlation process of the captured images is generally executed in three steps, as briefly described below.

The specimen's surface should be prepared for the DIC process in such a way that the captured digital images should have a suitable random speckle pattern. Therefore, the specimen should be painted white. After drying, the paint should be sprayed by a black mist of paint until a random speckle pattern is achieved. Finally, the specimen is fixed in the tensile testing machine (see

Figure 2). During testing, the (un)deformed images of the specimen are captured before and after deformation. These images are correlated for the calculation of the displacement fields. More details about this method are presented by Hild and Roux.<sup>32</sup>

## Experimental procedure

### Materials

The dissimilar DCB adhesive joints were made by bonding of CFRP and aluminium 7075-T6 substrates. For adhesive bonding, the structural epoxy adhesive Araldite 2011 (Huntsman, Basel, Switzerland) was used. The CFRP substrates were manufactured using the vacuum infusion technique where unidirectional T300 carbon fibres were added to reinforce the matrix. Araldite LY 5052 Resin and Aradur 5052 Hardener with a weight ratio of 100/38 (resin/hardener) were used as the matrix of the CFRP laminates. The CFRP laminate was cured according to the manufacturer datasheet, 1 day at 23 °C followed by 1 h at 100 °C. The mechanical properties of aluminium 7075-T6, CFRP laminates, Araldite 2011 adhesive are summarized in Table 1. To obtain these properties samples were manufactured with aluminium 7075-T6, CFRP and Araldite 2011 and tested according to ASTM E8, ASTM D3039 and ASTM D638, respectively. For each case, three specimens were prepared and tested.

### Geometry

Two kinds of specimens were fabricated and tested, including dissimilar DCB adhesive joints and CFRP substrates. The CFRP substrates were used to measure the effect of cyclic aging on the flexural stiffness and dissimilar DCB specimens with CFRP/aluminium substrates were used to calculate the variation of mode-mixity before and after aging. Figure 3 schematically shows the considered dissimilar DCBs with CFRP/aluminium substrates.

To accelerate the aging effect on the fracture properties of DCB specimens Costa et al.<sup>33</sup> proposed a mini DCB shown in Figure 3. They revealed that there is no significant difference in fracture energy obtained by the standard

**Table 1.** Mechanical properties of adhesive and substrates (subscript 1: longitudinal/fibre direction; subscript 2: transverse direction).

Material	$E_1$ (MPa)	$E_2$ (MPa)	$G_{12}$ (MPa)	$\nu_{12}$
UD-CFRP	81,000±5500	9350±700	8100±950	0.35
Aluminium 7076-T6	71,000±3500	—	—	0.33
Araldite 2011	1550±150	—	—	0.45

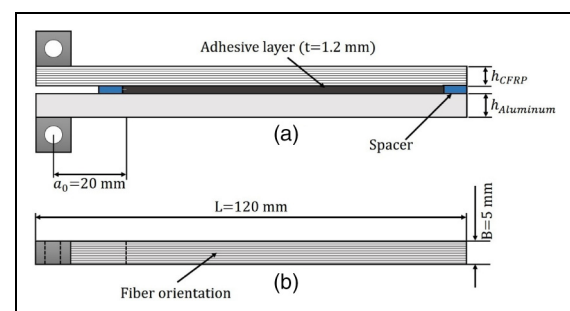


**Figure 3.** Schematic of a dissimilar double cantilever beam (DCB) specimen, (a) side view and (b) top view.

DCB with regular size and the tested mini DCBs. Therefore, in this research to accelerate the aging process, mini DCB specimens were manufactured and tested. For the CFRP substrates, after curing, the laminate was cut into samples of 5 mm by 120 mm. These dimensions of the DCB samples are based on the geometry of the mini DCB proposed by Costa et al.<sup>33</sup> The fibre orientation was along the substrate length (see Figure 3(b)). Some of these CFRP substrates were used as adherend to prepare dissimilar DCB specimens and some were aged without bonding and were tested in a three-point bending test setup. One side of these CFRP substrates was sealed with aluminium foil to prevent moisture absorption from the sealed surface.

As mentioned before, in a dissimilar DCB specimen, the achievement of pure mode I loading is challenging. In order to achieve a pure mode I loading in dissimilar DCB joints, the thickness of substrates was specified based on the longitudinal strain criterion (see equation (5)). This approach has been already verified using FEM simulations in dissimilar DCB adhesive joints including CFRP and GFRP substrates.<sup>16,19</sup>

$$E_{\text{Aluminium}} h_{\text{Aluminium}}^2 = E_{\text{CFRP}} h_{\text{CFRP}}^2 \quad (5)$$

where  $E$  denotes Young's modulus and  $h$  represents the thickness of the specimen.

The thickness of the aluminium and CFRP substrates were considered as 4 and 3.75 mm, respectively. It should be noticed that for the aluminium and CFRP substrates, the thickness tolerances were 0.05 and 0.2 mm, respectively.

### Joint manufacturing

For the manufacturing of dissimilar DCB adhesive joints, the bonded surfaces of the CFRP laminates were manually lightly sanded with 240 grit sandpaper without causing any damage to the fibres. Before and after sanding the surfaces were cleaned with acetone. For the aluminium surface treatment, all the bonded aluminium surfaces were grit blasted using aluminium oxide. During the grit blasting the air pressure was three bars and the grit blasting pistol was at a distance of 5 cm from the specimen surface with an angle of 30°. Before and after grit blasting, the aluminium surfaces were cleaned with a cloth soaked with acetone. Then the aluminium substrates were immersed in the sol-gel AC-130 (3M, Unitek) bath for 2 min, and then they were dried at ambient temperature for 60 min. Finally, primer EW-5005 (3M, Unitek) was sprayed on the aluminium surfaces using an airbrush, and the aluminium substrates were again dried at ambient conditions for 30 min and cured at 121 °C for

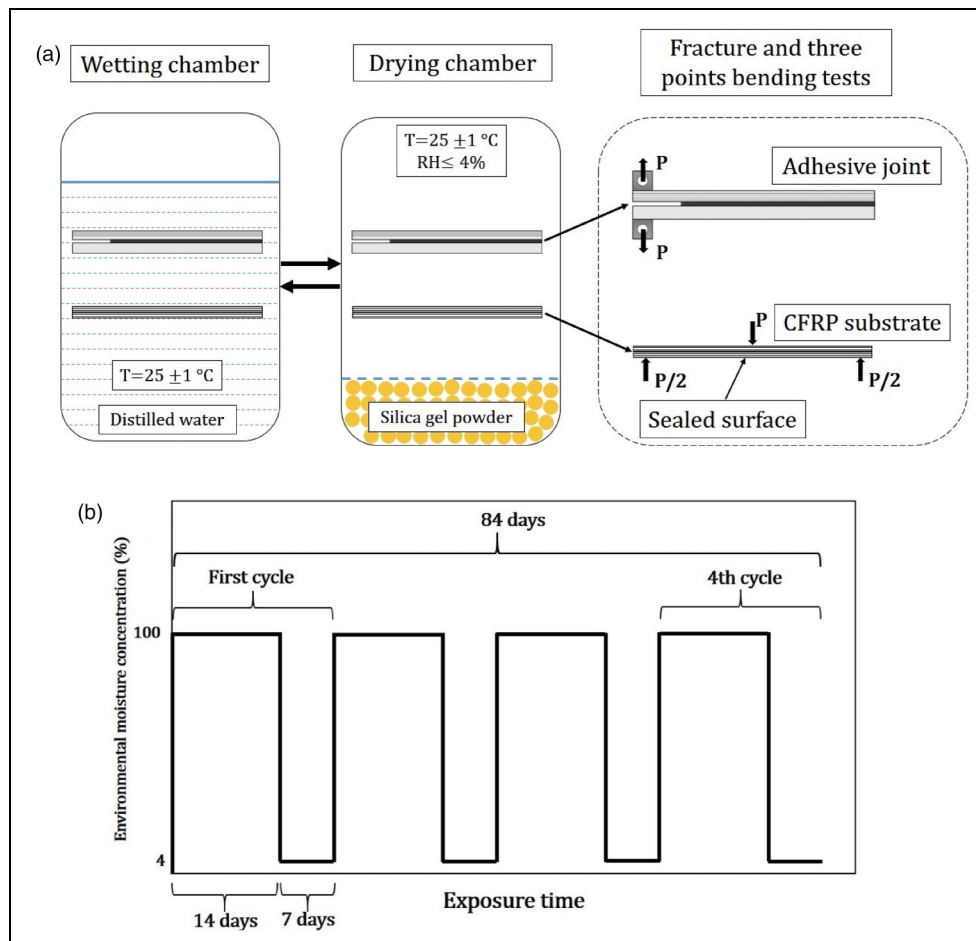


**Figure 4.** Schematic diagram of the aging conditions (a) and exposure time (b).



60 min. After the surface treatment, Araldite 2011 was mixed with a weight ratio of 100/80 (resin/hardener) using a mixer machine for 2 min at 2300 r/min. After mixing, the adhesive was applied by hand, using a syringe on the surfaces. The adhesive joints were cured for 40 min at 80 °C according to the manufacturer's technical datasheet. To control the thickness of the adhesive layer, spacers made of metal coated by a release agent were used on both sides of the DCB specimens. For all the specimens the thickness of the adhesive layer was 1.2 mm. In order to have enough input data for the over-deterministic technique used for the displacement fields obtained by the DIC method, the adhesive thickness considered in this study is more than the common adhesive layer thickness used in the literature. A sharp razor blade was used to make a pre-crack in the middle of the adhesive layer during the fabrication. Both the spacers and the razor blades were removed after curing and before testing (see Figure 3(a)).

### Test procedure

The fabricated specimens (dissimilar DCB adhesive joints and CFRP substrates) were exposed during 14 days by immersing the substrates in distilled water, followed by 7 days drying for each cycle, and for a total aging duration of 84 days, as shown in Figure 4(b). The aging and drying temperatures were both set to  $25 \pm 1$  °C. For the aging process, the substrates were immersed in distilled water while for the drying step the substrates were kept at a relative humidity of 4% for 7 days using a box containing silica gel powder. Each consecutive wetting-drying shows one cycle and this wetting-drying process was repeated 4 times (four cycles).

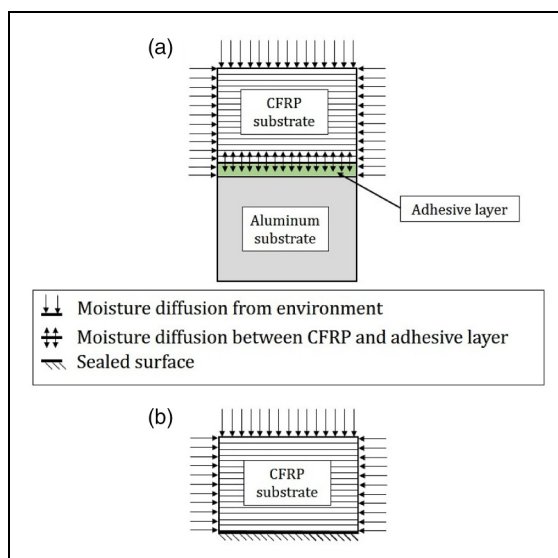


**Figure 5.** Moisture diffusion conditions in (a) double cantilever beam (DCB) adhesive joint and (b) carbon-fibre reinforced composites (CFRP) substrate sections.

In each cycle after the moisture absorption, some dissimilar DCB specimens and CFRP substrates were taken out of the distilled water and were tested in tensile and three-point bending, respectively. Figure 4(a) illustrates a schematic of aging conditions and fracture and three points bending tests.

In dissimilar DCB adhesive joints during the wetting and drying the moisture diffusion occurs in the CFRP substrate, adhesive layer and interface region. In CFRP substrates, the moisture absorption and desorption happens in three faces. Figure 5 shows the moisture diffusion conditions in dissimilar DCB adhesive joints and CFRP substrates.

A Zwick tensile test machine, equipped with a 1-kN load cell (precision of 0.5%) was employed to test the specimens. For dissimilar DCB adhesive joints, the fracture test was carried out under a constant displacement rate of 0.2 mm/min and for the CFRP substrates the displacement rate in three-point bending tests was set to 0.5 mm/min. The tests were carried out at laboratory conditions (temperature of 23 °C and relative humidity of 35%). Three repeats of each dissimilar DCB adhesive joint and CFRP substrates were tested.

DIC was used to measure the displacement fields near the crack tip during the fracture test. The obtained displacement fields were used to analyse the mode mixity of the DCB specimens. Digital camera images were captured continuously from the specimen's side surface with a constant rate of one picture every second. The DIC setup consisted of an 8-bit 'Point Grey' camera with a resolution of 5 MP, equipped with a 'XENOPLAN 1.4/23' lens. The software used for capturing the images was VIC-Snap 8, a product of 'Correlated Solutions Inc.' Using this setup, the resolution of the captured images was about  $2048 \times 2048$  pixels. The output from the tensile test machine was used to synchronize the captured images with their corresponding load and displacement at different measurement times. The DIC

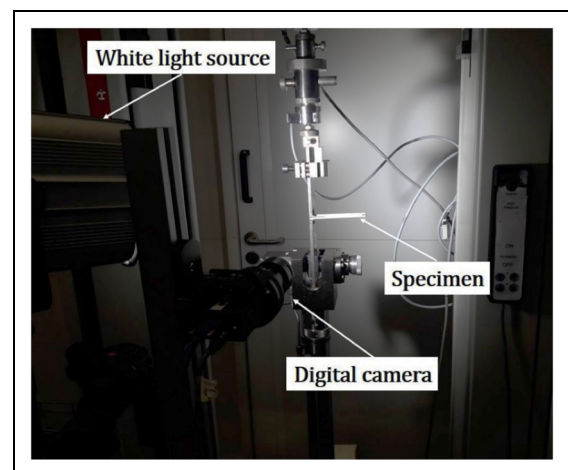


**Figure 6.** Experimental setup for the double cantilever beam (DCB) test.



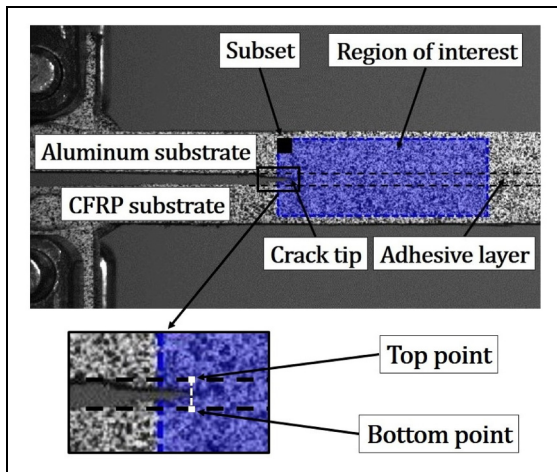


**Figure 7.** Region of interest on the surface of the double cantilever beam (DCB) specimens.

setup was installed at a distance of 65 cm from the specimen surface. Figure 6 illustrates the experimental setup.

After capturing images, the acquired data was processed using Vic-2D 6 software. A parametric study on the effect of the subset and step size on the displacement fields was performed. The subset and step size for the correlation process were defined as  $31 \times 31$  and 5 pixels, respectively. The region of interest in front of the crack tip including the adhesive layer was selected for calculation of the displacement fields. The region of interest and subset situation for DCB adhesive joints are presented in Figure 7.

The image of the deformed specimen was captured for all dissimilar DCB specimens, when the tensile load reached 50 N. Using the DIC approach, the displacement fields in the region of interest were measured. It should be noted that the obtained results of the DIC method are in the pixel unit and should be converted to mm. In the captured images each mm includes 52 pixels. This data

acquisition process was repeated for the dissimilar DCB specimens before aging and after the first, second and fourth aging cycles. The obtained results were used for an over-deterministic method and a comparison of the mode-mixity qualitatively. In this approach, the difference of the horizontal displacements between the top and bottom points in the adhesive layer at the  $x$ -location of the crack tip was measured in DCB adhesive joints (see Figure 7).

On the other hand, the CFRP substrates were tested under three points bending loading conditions before and after cyclic aging in order to simulate the moisture uptake of the CFRP substrates in the DCB joints. Using the test data, the variation of flexural stiffness as a function of aging cycles was obtained. As the sealed surface is used to mimic the adhesive surface in the DCB joints, in all the bending tests, the sealed surfaces were positioned at the bottom surface that experience tensile stresses (see Figure 4(b)). Before the test, the aluminium foil was removed from the CFRP specimens.

### Details of the FEM analysis

In the numerical process, the vertical and horizontal displacement fields of the dissimilar DCB specimens were calculated using Abaqus®. In the simulation section, the mechanical properties of the adhesive and substrates were defined according to Table 1. The 8-node biquadratic plane strain quadrilateral, reduced integration elements (CPE8R) were used during the simulation process. For the numerical simulation, Abaqus®/Standard solver was employed. Based on the mesh convergence analysis, a total number of 5340 elements were found to be sufficient in the adhesive layer for reaching mesh-independent results. Figure 8 represents the mesh pattern for the dissimilar DCB adhesive joints.

Figure 8 shows the boundary conditions applied in the FE simulation. To simulate the boundary conditions

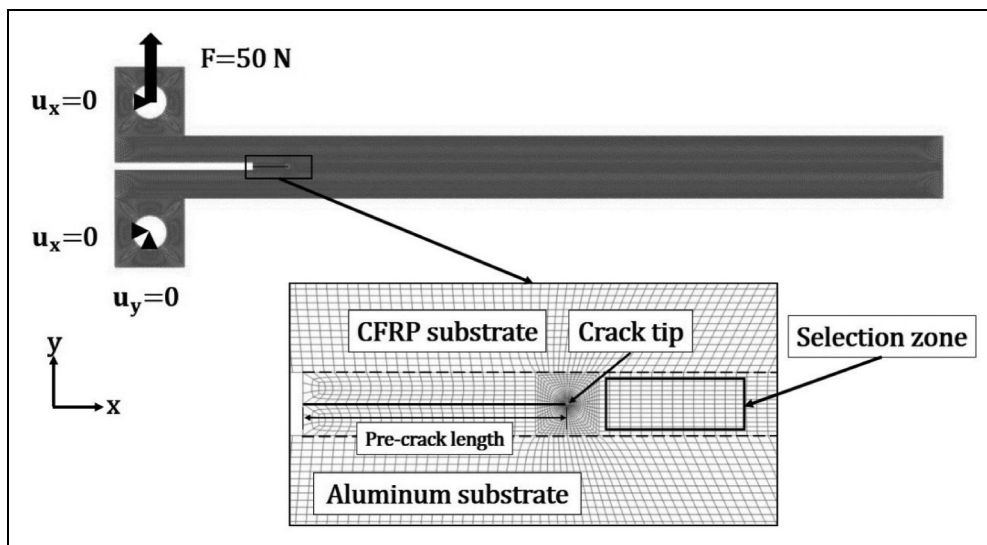


**Figure 8.** Fe mesh pattern in the dissimilar double cantilever beam (DCB) adhesive joints and selection zone.

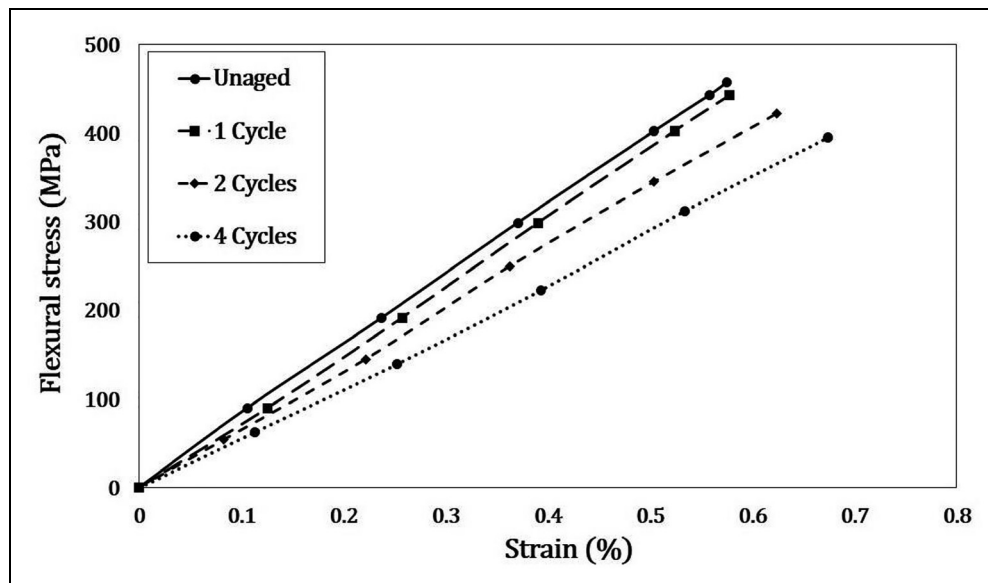


**Figure 9.** Flexural stress–strain curves for a different number of aging cycles for carbon-fibre reinforced composites (CFRP) specimens.

similar to the experimental tests, the centre point of the hole in the block bonded to the bottom substrate was constrained from all displacements. A tensile load was applied on the centre point of the hole of the top substrate. The displacement fields near the crack tip were obtained using a FE simulation under a 50 N tensile load. Then, the calculated displacement for the nodes near the crack tip was used as the input data for the over-deterministic approach. In this step, using the numerical developed code, the polar coordinates of the nodes in the adhesive layer near the crack tip were extracted and by fitting the Williams series expansion to the inputted data, the modes I and II SIFs were calculated numerically.

## Results and discussion

### Aging effects on the flexural stiffness of CFRP substrates

During these tests, using the DIC technique, the deflection of the specimens was calculated and the flexural stiffness of un-aged and aged substrates was measured based on ASTM D7264. Figure 9 shows the flexural stress–strain curves for CFRP substrates after a different number of aging cycles.

**Table 2.** Flexural modulus and strength for different aging conditions.

Aging conditions	Flexural modulus (GPa)	Flexural strength (MPa)
Un-aged	81.2 ( $\pm 2.3$ )	457 ( $\pm 15$ )
Aged (1 cycle)	74.6 ( $\pm 1.6$ )	443 ( $\pm 21$ )
Aged (2 cycles)	66.8 ( $\pm 3.2$ )	421 ( $\pm 23$ )
Aged (4 cycles)	56.8 ( $\pm 2.2$ )	394 ( $\pm 24$ )

As shown in Figure 9, cyclic aging affects the stress–strain curves and the amount of stiffness decreases with increasing aging cycles in the CFRP substrates. The Chord approach, which is defined in ASTM D7264, was used to measure the flexural modulus of the CFRP substrates. For calculation of the flexural Chord modulus, the considered strain range was 0.002 (starting at 0.001 and ending at 0.003). The flexural modulus in different aging conditions is reported in Table 2.

As can be concluded from Table 2, during the aging process the flexural modulus and strength of CFRP substrates decrease with increasing aging cycles. This trend was also observed by previous researchers.<sup>29</sup>

### Displacement fields analysis

For calculation of the displacement fields in un-aged and cyclically aged dissimilar DCB joints, the region of interest was defined in front of the crack tip. The horizontal (U) and vertical (V) displacement fields calculated from the DIC method in front of the crack tip under a tensile load of 50 N are illustrated in Figure 10.

As mentioned before, using the difference of horizontal displacement between the top and bottom interface (see Figure 6), the mode mixity of DCB can be investigated qualitatively.<sup>16,19</sup> In pure mode I DCB joints, the horizontal displacement at the top and bottom interface is the same, but in mixed-mode dissimilar DCB specimens, the adhesive layer experiences shear strain and the horizontal displacement changes along with the adhesive layer. The difference of the horizontal displacement between the top and bottom points in the adhesive/substrate interface for un-aged and aged DCB specimens is reported in Table 3.

As can be seen from Table 3, in the un-aged dissimilar DCB adhesive joint, the difference of the horizontal

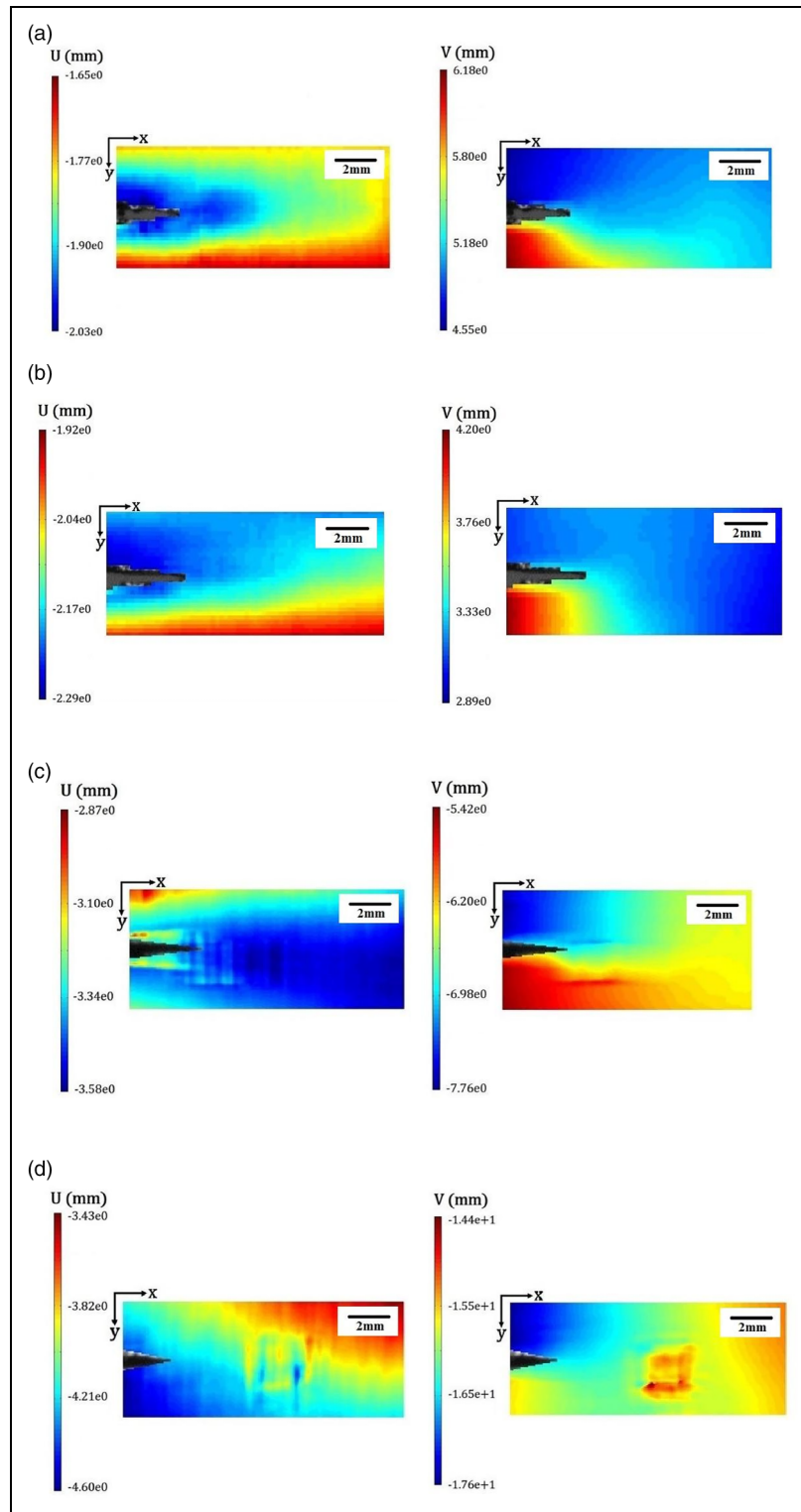


**Figure 10.** Typical horizontal (U) and vertical (V) displacement fields in front of the crack tip for un-aged (a) and cyclically aged double cantilever beam (DCB) specimen after one cycle (b), two cycles (c), and four cycles (d) aging.

displacement between top and bottom points in interfaces at the  $x$ -location of the crack tip is smaller than the aged specimen showing that un-aged specimen experiences more mode I loading in comparison with aged specimens. This result was expected because in the un-aged dissimilar DCB specimen the flexural stiffness of CFRP substrates is

equal to the initial stiffness which was considered during the design process following the longitudinal based strain design criterion.<sup>8</sup> The comparison of the results in Table 3 shows that the difference of the horizontal displacement between the top and bottom points of the adhesive increases with increasing aging cycles. Therefore, the

**Table 3.** Difference of the horizontal displacement between the top and bottom points.

Aging conditions	$ U_{Top} - U_{Bottom} $ (mm)
Un-aged	$0.36 \times 10^{-3} \pm 1.42 \times 10^{-4}$
Aged (1 cycle)	$3.26 \times 10^{-3} \pm 5.84 \times 10^{-4}$
Aged (2 cycles)	$4.18 \times 10^{-3} \pm 6.45 \times 10^{-4}$
Aged (4 cycles)	$6.43 \times 10^{-3} \pm 8.25 \times 10^{-4}$

amount of shear strain in the adhesive layer and mode II deformation increase after aging. According to the results in Table 3, the mode mixity of dissimilar DCB specimens increases with aging cycles due to the reduction in flexural stiffness of CFRP substrates after cyclic aging (see Figure 9).

### Verification of the over-deterministic approach

Before using the over-deterministic technique for calculation of the mode I and II SIFs, the numerical code developed based on this method was verified. To achieve this, the calculated mode I and II SIFs from the FE over-deterministic (FEOD) method were compared with SIFs calculated directly from the FE analysis. It should be noticed that in the FE analysis the flexural stiffness of the aged CFRP substrates was set as shown in Table 2. Table 4 represents and compares the calculated SIFs for un-aged and aged dissimilar DCB specimens under a tensile load of 50 N calculated using the FEOD technique and direct FE method.

As can be seen from Table 4, the mode I and II SIFs measured directly from the FEM and from the FEOD technique in un-aged and aged specimens are in very good agreement. The difference can be due to the possible numerical errors in the over-deterministic process. Therefore, the over-deterministic technique based on the Williams series expansion can be applied as an accurate approach in order to obtain the SIFs in dissimilar DCB adhesive joints, either from the displacement fields obtained from FE or DIC methods.

In addition, the comparison of the mode I and II SIFs obtained from FEOD and direct FEM for the un-aged and cyclically aged specimens shows that with the increase of aging cycles, the  $K_{II}/K_I$  ratio increases from 0.28% to 5.7%, and the dissimilar DCB specimens experience a higher mixed-mode level after cyclic aging. The maximum mode mixity, which is calculated

for the dissimilar DCB specimens after four aging cycles is smaller than 7%. In this aging condition, the flexural stiffness of CFRP substrates decreases to 70% of the flexural stiffness of un-aged specimens. However, after four aging cycles, the dissimilar DCB specimens experience a mode mixity very close to the mode I condition and mode II loading can be ignored after cyclic aging. As a result, despite the significant effect of cyclic aging on the flexural stiffness of the CFRP substrates, the mode mixities of aged dissimilar DCB specimens are close to zero and these specimens can be considered as a mode I DCB specimen. It should be noted that in the FE analysis the effect of aging on the elastic modulus of the adhesive layer was not simulated and for all the un-aged and aged DCB specimens, the mechanical properties of un-aged adhesive were assigned to the adhesive layer (see Table 1). Previous investigations<sup>34–36</sup> show that moisture diffusion decreases the elastic modulus of the adhesive materials and makes them more ductile. In the DCB specimen simulation, with a decrease of the elastic modulus of the adhesive layer, the mode I and II SIFs decrease as well, but the  $K_{II}/K_I$  ratio does not change significantly with the variation of elastic modulus of the adhesive layer. On the other hand, for the dissimilar DCB specimens, the moisture diffusion into the heart of the adhesive layer takes a long time from the side surface of the adhesive and this moisture diffusion affects the adhesive layer properties considerably.

### SIFs calculation DICOD method

In the previous section, the numerical code developed in this study using the over-deterministic method based on the Williams series expansion was verified. After the validation of the numerical code, the mode I and II SIFs in the un-aged and cyclically aged dissimilar DCB specimens were obtained. They were based on the displacement field measured from the DIC technique. Figure 11 represents the values of SIFs measured for un-aged and aged dissimilar DCB adhesive joints when the tensile load reached 50 N using the DICOD and FEOD methods.

As can be seen in Figure 11, in the un-aged dissimilar DCB joints, the  $K_{II}/K_I$  ratio obtained from DICOD, which shows the amount of mode mixity, is not zero. This mode mixity obtained from DICOD can be the result of experimental and numerical errors. Experimental errors such as in the CFRP substrate and the dissimilar DCB joint fabrication and numerical

**Table 4.** Mode I and II SIFs were calculated using the FEOD technique and the direct approach using the FEM.

Aging conditions	FEOD			FEM (direct)		
	$K_I$ (MPa $\sqrt{\text{mm}}$ )	$K_{II}$ (MPa $\sqrt{\text{mm}}$ )	$\frac{K_{II}}{K_I}$ (%)	$K_I$ (MPa $\sqrt{\text{mm}}$ )	$K_{II}$ (MPa $\sqrt{\text{mm}}$ )	$\frac{K_{II}}{K_I}$ (%)
Un-aged	14.95	0.06	0.44	15.87	4.42e-2	0.28
Aged (1 cycle)	17.26	0.31	1.81	16.12	0.17	1.05
Aged (2 cycles)	17.54	0.82	4.66	16.46	0.48	2.92
Aged (4 cycles)	16.68	1.07	6.43	17.01	0.97	5.70

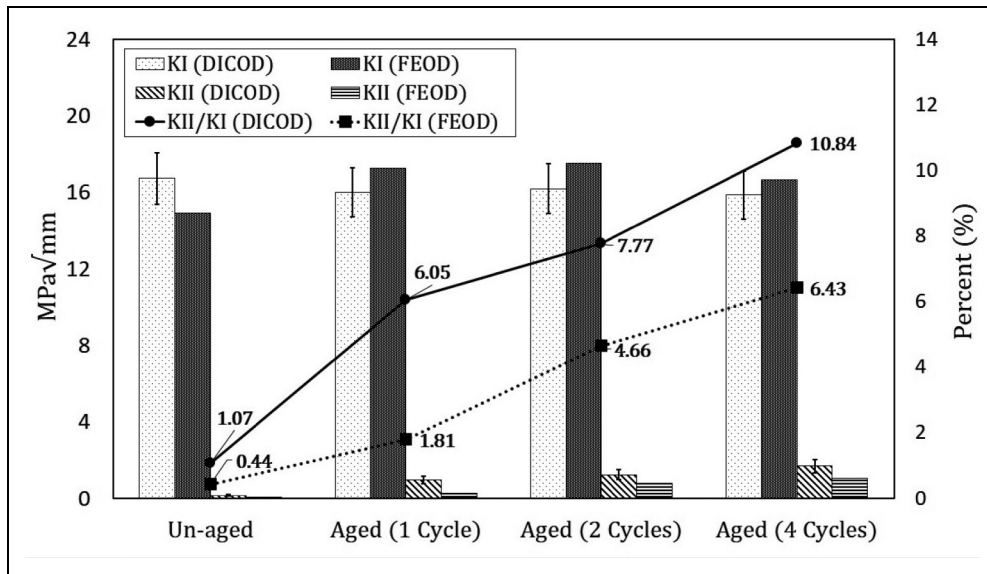


**Figure 11.** Mode I and II SIFs were obtained using the DICOD and FEOD methods. DICOD: digital image correlation over-deterministic; FEOD: finite element over-deterministic.

errors during the calculation of displacement fields using image correlation and over-deterministic technique can affect the  $K_{II}/K_I$  ratio. As expected, the results in Figure 11 show that the mode-mixity ratio of the aged dissimilar DCB adhesive joints obtained from different methods increases with aging cycles. The  $K_{II}/K_I$  ratio based on DIC results for the DCB specimens after four cycles of aging reaches 10.84%. The comparison of the  $K_{II}/K_I$  ratios obtained from DICOD and FEOD techniques show that in all dissimilar DCB adhesive joints the mode mixity obtained using the DICOD method is bigger than the FEOD results. For instance, in the dissimilar DCB specimen after four cycles of aging, the  $K_{II}/K_I$  ratios obtained from DICOD and FEOD methods are 10.84% and 6.43%, respectively. It should be mentioned that the numerical code which is used for the FEOD and the DICOD methods is the same. Therefore, the difference in the  $K_{II}/K_I$  ratio obtained from DICOD and FEOD is possibly due to the difference in the displacement fields obtained through the DIC approach and FEM. As mentioned before, for un-aged and aged dissimilar DCB specimens there are some experimental errors such as errors in the CFRP and DCB fabrication and test procedures, which affect the displacement fields during the mode I fracture test. In the aged dissimilar DCB adhesive joints there are some residual stresses in the adhesive layer and within the CFRP substrates induced by the moisture swelling. In CFRP laminates, the moisture-induced dimensional swelling along the fibre direction is significantly smaller than in other directions and the swelling creates a small expansion along the fibre direction.<sup>37</sup> Because of the limitation in dimensional swelling of CFRP substrates along the fibre direction, some residual stresses are induced in the CFRP and the adhesive layer, simultaneously. The residual stresses can affect the displacement fields in front of the crack tip during the tensile test and change

the mode mixity of the specimens. Based on the obtained results, the maximum difference of the  $K_{II}/K_I$  ratio as a result of swelling in the aged specimens after four cycles of aging is about 4%. Another reason for the difference in the displacement fields obtained from DIC and FEM is the effect of moisture diffusion on the mechanical properties of the adhesive layer, which were not taken into account. As mentioned before, these parameters decrease mode I and II SIFs and change the mode mixity. On the other hand, during the aging process, moisture diffusion can occur from the adhesive layer to the CFRP substrates. Therefore, in reality, the CFRP absorbs a small amount of moisture from the adhesive layer and this parameter was not considered in the numerical simulation.

## Conclusion

In this paper, using experimental and numerical techniques, the effect of cyclic aging on the mode mixity of dissimilar DCB adhesive joints was studied. For this purpose, DCB joints with CFRP-aluminium substrates were made and exposed to cyclic aging. Then, the unaged and cyclic aged specimens were tested under tensile load. During the tensile tests, the displacement fields were measured using the DIC method. Using an over-deterministic approach based on the Williams series expansions and by considering the DIC results, mode I and II SIFs for unaged and aged specimens were calculated for different numbers of aging cycles. On the other hand, through three-point bending tests, the variation in flexural stiffness of CFRP substrates was measured as a function of aging cycles. To verify the results of the over-deterministic method, in the numerical section, joints were simulated using FEM. The SIF values obtained directly from the FE analysis were compared with the results of the FEOD technique.

According to the obtained results, the following points can be concluded:

- The flexural stiffness of the CFRP substrates decreases significantly after cyclic aging, and with increasing aging cycles the flexural stiffness decreases continually. The obtained results show that the flexural stiffness of CFRP substrates that were aged during four cycles is 70% of the flexural stiffness of un-aged specimens.
- In the dissimilar DCB adhesive joints with the CFRP substrate, the  $K_{II} / K_I$  ratio increases with increasing aging cycles, and this parameter reaches 10.84% after four cycles of aging. This shows that the adhesive layer experiences more shear strain with increasing aging cycles.
- The difference of the horizontal displacement between the top and bottom interface of the adhesive layer can be used as a primary parameter for comparison of the mode mixity in un-aged and aged dissimilar DCB specimens. When the mode mixity increases, the value of this parameter increases.
- In general, the  $\frac{K_{II}}{K_I}$  ratio calculated from the experimental tests is higher than the numerical results and this difference can be the result of experimental errors, such as residual stress created by swelling in the CFRP substrates, the effect of aging on the mechanical properties of the adhesive layer and/or moisture diffusing from the adhesive layer to the CFRP substrates.
- The comparison of the numerical and experimental results show that the difference of the  $K_{II} / K_I$  ratio calculated from the experimental and numerical sections increase with increasing aging cycles, which can be the result of increasing the residual stress in the CFRP substrates and/or the effect of moisture diffusion into the adhesive layer during the cyclic aging.




### Declaration of conflicting interests

The authors declared no potential conflicts of interest with respect to the research, authorship, and/or publication of this article.

### Funding

The authors received no financial support for the research, authorship and/or publication of this article.

### ORCID iDs

Majid R Ayatollahi  <https://orcid.org/0000-0001-9840-6225>  
 Johannes A Poulis  <https://orcid.org/0000-0003-3041-5285>  
 Lucas FM da Silva  <https://orcid.org/0000-0003-3272-4591>

### References

1. Mouritz AP, Gellert E, Burchill P, et al. Review of advanced composite structures for naval ships and submarines. *Compos Struct* 2001; 53: 21–42.
2. Passos A, Arouche M, Aguiar R, et al. Adhesion of epoxy and polyurethane adhesives in pultruded composite material. *J Adv Joining Process* 2021; 3: 100045.
3. Budhe S, Banea M, De Barros S, et al. An updated review of adhesively bonded joints in composite materials. *Int J Adhesion Adhes* 2017; 72: 30–42.
4. de Freitas ST, Banea M, Budhe S, et al. Interface adhesion assessment of composite-to-metal bonded joints under salt spray conditions using peel tests. *Compos Struct* 2017; 164: 68–75.
5. Wang W, De Freitas ST, Poulis JA, et al. A review of experimental and theoretical fracture characterization of bi-material bonded joints. *Compos B, Eng* 2020; 206: 108537.
6. Zheng G, Wang H, Han X, et al. Mechanical behavior of AL/CFRP single-lap joint subjected to combined thermal and constant loading. *J Adhes* 2021; 97: 361–379.
7. Akhavan-Safar A, Ayatollahi M, Safaei S, et al. Mixed mode I/III fracture behavior of adhesive joints. *Int J Solids Struct* 2020; 199: 109–119.
8. Ajdani A, Ayatollahi MR, Akhavan-Safar A, et al. Mixed mode fracture characterization of brittle and semi-brittle adhesives using the SCB specimen. *Int J Adhes Adhes* 2020; 101: 102629.
9. Akhavan-Safar A, Beygi R, Delzendehrooy F, et al. Fracture energy assessment of adhesives—part I: is GIC an adhesive property? A neural network analysis. *Proceedings of the Institution of Mechanical Engineers, Part L: Journal of Materials: Design Applications* 2021; 235: 1461–1476.
10. Leplat J, Stamoulis G, Bidaud P, et al. Investigation of the mode I fracture properties of adhesively bonded joints after water ageing. *J Adhes* 2020; 98: 1–22.
11. Delzendehrooy F, Beygi R, Akhavan-Safar A, et al. Fracture energy assessment of adhesives part II: is GIIC an adhesive material property? (a neural network analysis). *J Adv Joining Process* 2021; 3: 100049.
12. Bin Mohamed Rehan MS, Rousseau J, Fontaine S, et al. Experimental study of the influence of ply orientation on DCB mode-I delamination behavior by using multidirectional fully isotropic carbon/epoxy laminates. *Compos Struct* 2017; 161: 1–7.
13. Shokrieh MM, Heidari-Rarani M and Ayatollahi MR Interlaminar fracture toughness of unidirectional DCB specimens: a novel theoretical approach. *Polym Test* 2012; 31: 68–75.
14. Fevery S, Hallez H, Vandepitte D, et al. Lifetime assessment of structural adhesive joints by combining effects of mechanical load, humidity, moisture and UV: design of a test rig. *J Adhes* 2020; 96: 461–473.
15. Khoshnavan M and Asgari Mehrabadi F. Fracture analysis in adhesive composite material/aluminum joints under mode-I loading; experimental and numerical approaches. *Int J Adhes Adhes* 2012; 39: 8–14.
16. Wang W, Fernandes RL, De Freitas ST, et al. How pure mode I can be obtained in bi-material bonded DCB joints: a longitudinal strain-based criterion. *Compos B, Eng* 2018; 153: 137–148.
17. Boeman RG, Erdman D, Klett L, et al. *A practical test method for mode I fracture toughness of adhesive joints with dissimilar substrates*. Oak Ridge, TN: Oak Ridge National Laboratory (ORNL), 1999.
18. Jiang Z, Wan S and Wu Z. Calculation of energy release rate for adhesive composite/metal joints under mode-I loading considering effect of the non-uniformity. *Compos B, Eng* 2016; 95: 374–385.
19. Moazzami M, Ayatollahi M, de Freitas ST, et al. Towards pure mode I loading in dissimilar adhesively bonded double cantilever beams. *Int J Adhes Adhes* 2021; 107: 102826.



20. Ayatollahi M and Nejati M. An over-deterministic method for calculation of coefficients of crack tip asymptotic field from finite element analysis. *Fatigue Fracture Eng Mater Struct* 2011; 34: 159–176.
21. Chalmers D. The potential for the use of composite materials in marine structures. *Marine Struct* 1994; 7: 441–456.
22. Starkova O, Buschhorn ST, Mannov E, et al. Water transport in epoxy/MWCNT composites. *Eur Polym J* 2013; 49: 2138–2148.
23. Becker O, Varley RJ and Simon GP. Thermal stability and water uptake of high performance epoxy layered silicate nanocomposites. *Eur Polym J* 2004; 40: 187–195.
24. Han SO and Drzal LT. Water absorption effects on hydrophilic polymer matrix of carboxyl functionalized glucose resin and epoxy resin. *Eur Polym J* 2003; 39: 1791–1799.
25. Eslami S, Taheri-Behrooz F and Taheri F. Effects of aging temperature on moisture absorption of perforated GFRP. *Adv Mater Sci Eng*. 2012; 2012: 303014.
26. Newman RH. Auto-accelerative water damage in an epoxy composite reinforced with plain-weave flax fabric. *Compos Part A: Appl Sci Manuf* 2009; 40: 1615–1620.
27. Bond DA. Moisture diffusion in a fiber-reinforced composite: part I–non-fickian transport and the effect of fiber spatial distribution. *J Compos Mater* 2005; 39: 2113–2141.
28. Suri C and Perreux D. The effects of mechanical damage in a glass fibre/epoxy composite on the absorption rate. *Compos Eng* 1995; 5: 415–424.
29. Gassan J and Bledzki AK. Effect of cyclic moisture absorption desorption on the mechanical properties of silanized jute-epoxy composites. *Polym Compos* 1999; 20: 604–611.
30. Houjou K, Shimamoto K, Akiyama H, et al. Effect of cyclic moisture absorption/desorption on the strength of epoxy adhesive joints and moisture diffusion coefficient. *J Adhes* 2021; 118: 1–17.
31. Williams M. On the stress distribution at the base of a stationary crack. *Mech* 1957; 24: 109–114.
32. Hild F and Roux S. Measuring stress intensity factors with a camera: integrated digital image correlation (I-DIC). 2006.
33. Costa M, Viana G, Canto C, et al. Effect of the size reduction on the bulk tensile and double cantilever beam specimens used in cohesive zone models. Proceedings of the institution of mechanical engineers. *Part L: J Mater: Desig Appl* 2016; 230: 968–982.
34. Moazzami M, Ayatollahi M, Akhavan-Safar A, et al. Experimental and numerical analysis of cyclic aging in an epoxy-based adhesive. *Polym Test* 2020; 91: 106789.
35. Da Costa J, Akhavan-Safar A, Marques E, et al. Effects of cyclic ageing on the tensile properties and diffusion coefficients of an epoxy-based adhesive. *Proceedings of the Institution of Mechanical Engineers, Part L: Journal of Materials: Design Applications* 2021; 235: 1451–1460.
36. Da Costa J, Akhavan-Safar A, Marques E, et al. Cyclic ageing of adhesive materials. *J Adhes* 2021; 130: 1–17.
37. Kumar S, Sridhar I and Sivashanker S. Influence of humid environment on the performance of high strength structural carbon fiber composites. *Mater Sci Eng: A* 2008; 498: 174–178.